

Design of fast adaptive readout system for wire scanners

Qian-Shun She^{1,2} · Yi Qian¹ · Jie Kong¹ · Hai-Bo Yang¹ · Hong-Yun Zhao¹ ·
Jing-Zhe Zhang¹ · Xiao-Yang Niu^{1,2} · Jun-Xia Wu¹ · Hong Su¹

Received: 29 November 2016 / Revised: 20 April 2017 / Accepted: 29 April 2017 / Published online: 29 December 2017
© Shanghai Institute of Applied Physics, Chinese Academy of Sciences, Chinese Nuclear Society, Science Press China and Springer Nature Singapore Pte Ltd. 2017

Abstract A new wide-range fast readout system capable of adaptive identification is designed for wire scanners, which are used to measure beam profiles and emittance. This system is capable of handling varying current signals with Gaussian distributions and current pulses up to 1000 counts/s, as well as an input current range of 1 nA–1 mA. When tested, the resolution was found to exceed 3.68% for full scale, the nonlinearity was found to be less than 0.11%, and the measurement sensibility was found to be less than 5 pA. We believe that the system will play a crucial role in improving the measurement accuracy of beam diagnosis and the efficiency of accelerator operation, as well as decreasing the time required for beam tuning. This system was applied to the beam diagnosis of an injector II prototype for an accelerator-driven subcritical system and produced excellent measurement results. A description of the adaptive fast readout system for wire scanners is presented in this paper.

Keywords Wire scanner · Weak current measurement · Adaptive identification · Front-end readout electronics · Beam diagnosis

1 Introduction

With improvement in the subsystems used in the Heavy Ion Research Facility of Lanzhou (HIRFL), the number of experimental terminals within this large scientific facility is increasing. Thus, it is possible to conduct more experiments at this facility; consequently, the requirements for beam quality are observed to increase as well. At the same time, the beams must be tuned according to the research requirements, because different research experiments require different beam types and energy ranges. In order to meet these various requirements and obtain better experimental data of nuclear physics research, the type and number of detectors for beam diagnosis have increased [1], and a large number of wire scanners must be used to measure the beam profiles and emittance [2]. The output current signal from a wire scanner often varies within a large range and is typically beyond the range of generic front-end electronic systems [3]. In order to cope with this dilemma, electronic systems with different ranges are generally adopted to prevent data points falling beyond the system's range from being lost, which significantly reduces the efficiency and accuracy of the beam diagnosis [4]. Meanwhile, staff members must pass through the experimental halls in order to exchange the measurement equipment, thereby increasing their risk of exposure to radiation. Furthermore, most of the real-time front-end readout circuits currently used only have the capacity to measure current varying within two to three orders of magnitude [5, 6], even though the current-to-voltage conversion circuits based on logarithmic amplifiers are capable of processing a current signal up to nine orders of magnitude [7]. Furthermore, these circuits are only suitable for detecting the average or relatively constant current and

This work was supported by the National Natural Science Foundation of China (Nos. 11475233, 11705257, and 11775285).

✉ Hong Su
suhong@impcas.ac.cn

¹ Institute of Modern Physics, Chinese Academy of Sciences, Lanzhou 730000, China

² University of Chinese Academy of Sciences, Beijing 100049, China

cannot analyze dynamic current signals in detail. In particular, when a current signal exceeding three orders of magnitude needs to be processed, the range of the readout electronics must be switched manually both at home and abroad [8], which severely affects the timeliness of the entire readout system. In order to meet the demands of readouts for wire scanners in beam diagnosis, there are important scientific significance and practical value to designing and developing an adaptive readout system with a wide measurement range for acquiring beam information. It will play an important role in improving the efficiency, utilization of HIRFL, and the accuracy of nuclear physics experiments.

Three subsequent sections comprise this paper. The first presents a detailed description of the proposed system. The second describes the testing along with the experimental results. Finally, a conclusion of the investigation is given.

2 System design

The fast adaptive readout system is mainly composed of three parts: a detector, front-end readout electronics, and a data acquisition system. A detailed description is presented in this section.

3 Detector

The wire scanner for the measurement of the beam profile and emittance in a diagnosis system is mainly composed of a fixed base and a movable expansion link [9, 10], which can travel along a guide rail on the base, under the control of a motor and with a maximum speed of 1 m/s. The structure of the wire scanner and the head of the expansion link are shown in Fig. 1. The expansion link is completely sealed within the beam pipe, which is fixed to a taut wire at a central position [11], and the diameter of the carbon wire is 30 μm [12]. Each side of the taut wire has a scraper plate, which is surrounded by water-cooling pipes. The wire and two scraper plates output a current signal. Through theoretical calculations and preliminary testing, the diameter through the wire scanner was determined to be 40 mm [13], the speed of the expansion link was designed

to be 1 m/s, the width of the current signal from the wire with a Gauss distribution was determined to be 40 ms when the beam is completely scanned, and the range of the signal was determined to be 1 nA–1 mA.

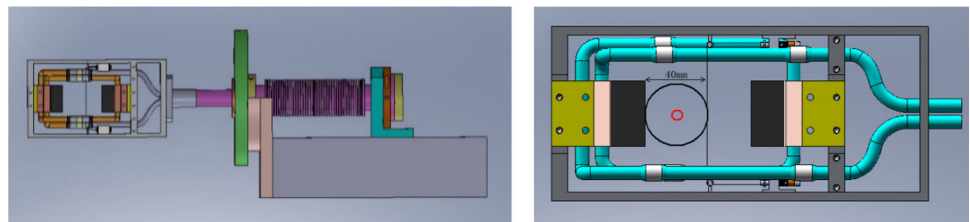
3.1 Front-end readout electronics

The design of a fast readout system with adaptive identification and a wide-scale range for a wire scanner is shown in Fig. 2. The system is composed of three key parts: current-to-voltage conversion circuits, adaptive identification circuits, and ultra-high-speed switching control circuits. There are three input channels in the system for processing current signals from the wire and scraper plates of beam separately. The input current ranges from 1 nA to 1 mA, with six orders of magnitude. Figure 2 shows the basic circuit structures only of channels 1 and 3, but the circuit structure of channel 2 is the same.

3.1.1 Current-to-voltage conversion circuit

The current-to-voltage conversion circuit in each input channel is composed of three current-to-voltage converters (IVCs) with different conversion gains for different measurement ranges: high range C, middle range B, and low range A, covering six orders of magnitude from 1 nA to 1 mA. Each IVC comprises an operational amplifier OP, a T-type feedback resistor network R_{FX} (here x equals A, B, or C), a low-pass filter (LPF), and a pair of high-speed switches SA_x , SB_x , or SC_x (here x equals 1 or 2). Since several precision resistors must be employed to construct a T-type resistor network in place of a single large resistor, R_{FX} with smaller errors is utilized. There are three pairs of high-speed analog switches in each input channel for switching between the different IVCs corresponding to the different measurement ranges depending on the control signals from the ultra-high-speed switching control circuit. These IVCs have the characteristics of low noise, high conversion accuracy, and are capable of precision compensation.

Fig. 1 (Color online) Structure of the wire scanner and head of the expansion link



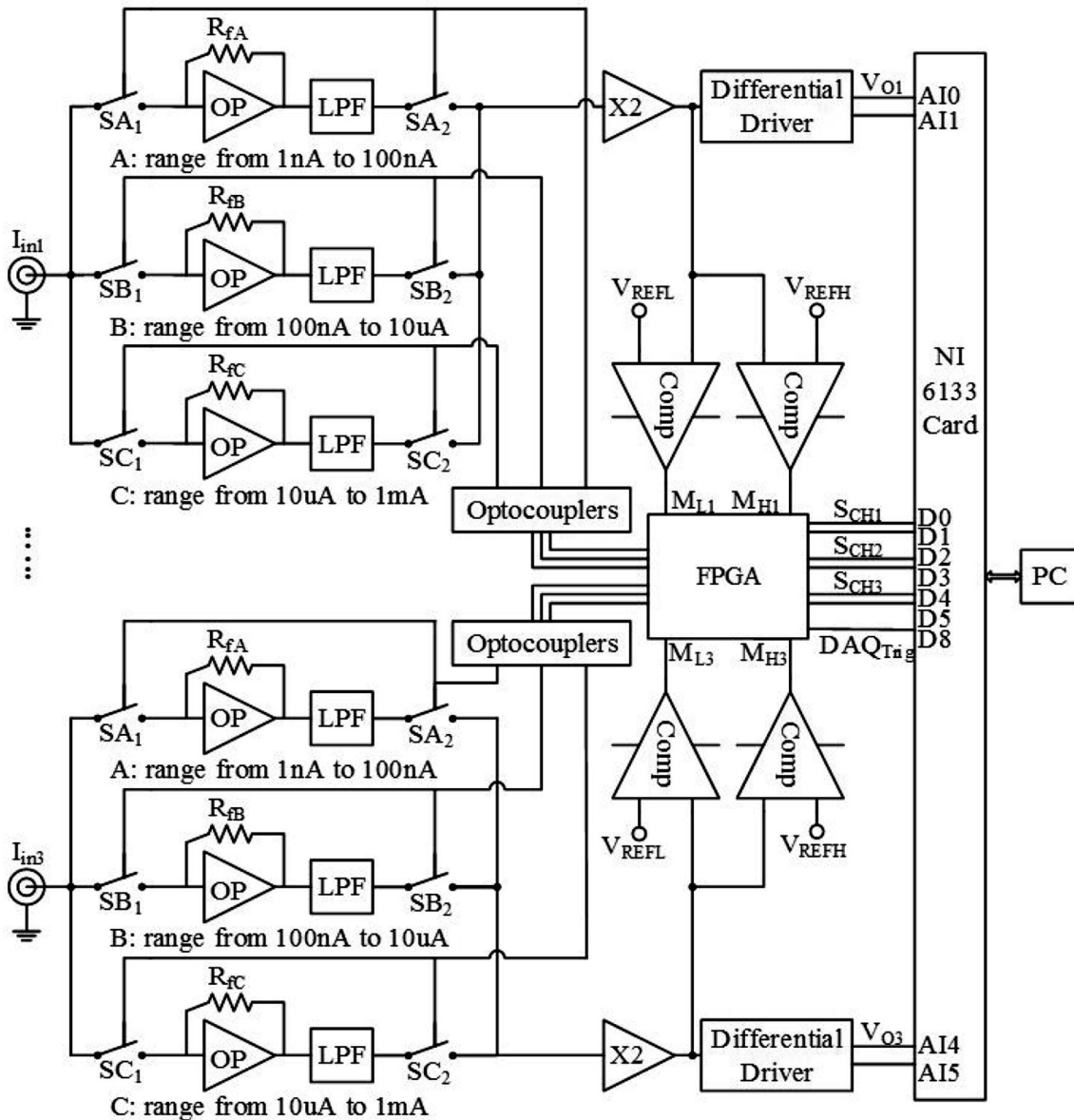


Fig. 2 Design of the front-end readout system

3.1.2 Adaptive identification circuit

The adaptive identification circuits are another key component of this system. There is an adaptive identification circuit in each channel. It consists of a main amplifier with a gain of 2, two high-speed comparators with a low threshold V_{REFL} and a high threshold V_{REFH} , and a differential driver. The two high-speed comparators are adopted to compare the output voltages of the IVCs with the thresholds set for identifying the input range. The logic and algorithm for identifying the input range are contained within a field-programmable gate array (FPGA). The output voltage signal from the current-to-voltage conversion circuit is amplified by the main amplifier first

and then fed into the comparators and differential driver simultaneously. The output voltage signal of the main amplifier is compared with the thresholds of the comparators, and the comparators produce an identification signal M_{Lx} or M_{Hx} (here x equals 1, 2, or 3) corresponding to the input range. The identification signals M_{Lx} and M_{Hx} are fed into the FPGA, in which the logic and algorithm for identifying the input range implement the identification of the input ranges. In other words, the logic and algorithm for identifying the input range in the FPGA can determine whether the input signal belongs to the selected measurement range by the identification signals M_{Lx} and M_{Hx} , and complete the adaptive identifying the range of input current. Other, the differential drive circuit converts the

single-ended voltage signal to a differential signal V_{Ox} (here x equals 1, 2, or 3) for improving ability of anti-jamming and feeds differential signal V_{Ox} into the data acquisition card. In order to realize fast adaptive identification of the input current range, the logic and algorithm are designed to scan the output voltage of the current-to-voltage conversion circuit from high to low voltage range and simultaneously compare it with the preset high threshold V_{REFHx} and low threshold V_{REFLx} (here x equals 1, 2, or 3) using the comparators. The two identification signals M_{Hx} and M_{Lx} fed into FPGA are designed to express three states: The first state is that the input current is within the measurement range selected, the second state is that the input current is larger than the maximum value of the measurement range selected, and the third state is that the input current is less than the value of the measurement range selected. According to these two identification signals M_{Hx} and M_{Lx} , the logic and algorithm for identifying the input range in the FPGA can perform an assessment and drive the appropriate switches to enact the range change.

3.1.3 Ultra-high-speed switching control circuit

The ultra-high-speed switching control circuit is developed based on the FPGA. There are three control signals from the FPGA for each input channel, which are fed to each IVC of the current-to-voltage conversion circuits in the channel via an opto-coupler to control the corresponding high-speed switch pair SA_x , SB_x , or SC_x for selecting the corresponding measurement range. The control circuit outputs three S_{CHx} (here x equals 1, 2, or 3) signals and a DAQ_{Trig} signal to the data acquisition part (DAQ) according to the logic and algorithm. When the S_{CHx} signal is valid, an output request signal of the corresponding channel is sent to the data acquisition part. The DAQ_{Trig} signal is the acquisition trigger signal; when it is valid, the DAQ begins to acquire data from the corresponding input channel.

3.1.4 Timing sequence of the control logic module

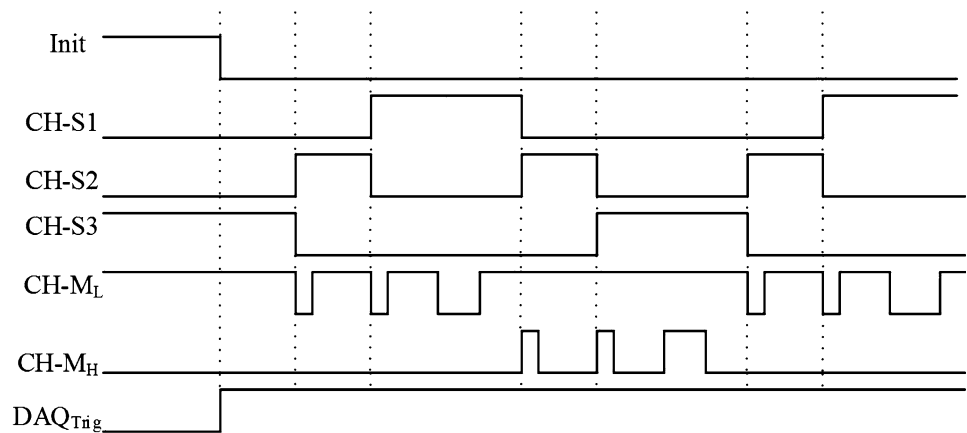
The timing sequence of the control logic module for each channel of this system is shown in Fig. 3. When the power supply is switched on, the signal “Init” is high, the system is initialized, the middle measurement range is set, and other measurement ranges remain idle. After initialization, the system is ready to measure the beam information. If the input current is in the measurement range selected, i.e., the output voltage of the current-to-voltage conversion circuit is greater than the low threshold V_{REFLx} of the comparator and less than the high threshold V_{REFHx} of the comparator, the $CH-M_L$ becomes high, and the $CH-$

M_H becomes low. The circuit continues to work in this range, and the DAQ card can acquire data. If the input current is greater than the maximum value of the selected range, which means the output voltage exceeds the high threshold V_{REFHx} of the comparator, then the $CH-M_L$ and $CH-M_H$ both become high, and a higher measurement range is selected by switching the pair of high-speed analog switches SA_x , SB_x , and SC_x of the adjacent IVCs with a high measurement range. If the input current is less than the minimum value of the selected range, which means the output voltage is less than the low threshold V_{REFLx} of the comparator, then the $CH-M_L$ and $CH-M_H$ both become low, and the low measurement range is selected by switching the pair of high-speed analog switches SA_x , SB_x , and SC_x of the adjacent IVCs with a low measurement range. In order to reduce the dead time caused by exchanging the switches of the IVCs, the ultra-high-speed DMOS analog switches are used to switch the IVCs with different measurement ranges. The switch time of a single switch is less than 20 ns, so the pulse width of the control signal is a maximum of 40 ns, required to set up a stable state of the switch. At this time, the statuses of the $CH-M_L$ and $CH-M_H$ are invalid.

In order to reduce noise, prevent interference, and maintain high accuracy in the case of a weak signal, special accommodations are incorporated into the front-end readout electronic circuit design. Firstly, electronic devices with low noise, low power, low bias current, and low offset voltage are selected. Secondly, special design methods are used to prevent current leakage and enhance the ability of anti-interference to improve the conversion accuracy. Thirdly, other techniques are used to design the shielding box of the circuit including increasing the thickness of the shielding box according to calculations, using concave and convex designs for the mouth to connect to the box body and cover plates, and choosing connectors and cables with excellent shielding performance. Such methods effectively optimize the performance of the front-end readout circuit.

3.2 Data acquisition system

The high-speed data acquisition system consists of a commercial DAQ card (PCI-6133) from National Instruments Corporation and an industrial computer shown as the PC in Fig. 2. The software of the data acquisition system was designed using the LabVIEW software platform [14]. The DAQ card mainly receives analog differential voltage signals V_{Ox} from three channels using the front-end electronics and implements sampling, analog digital conversion, and data acquisition. The PC displays the operation status of the three input channels, stores, and displays the data from the DAQ card, controls the motors of the wire

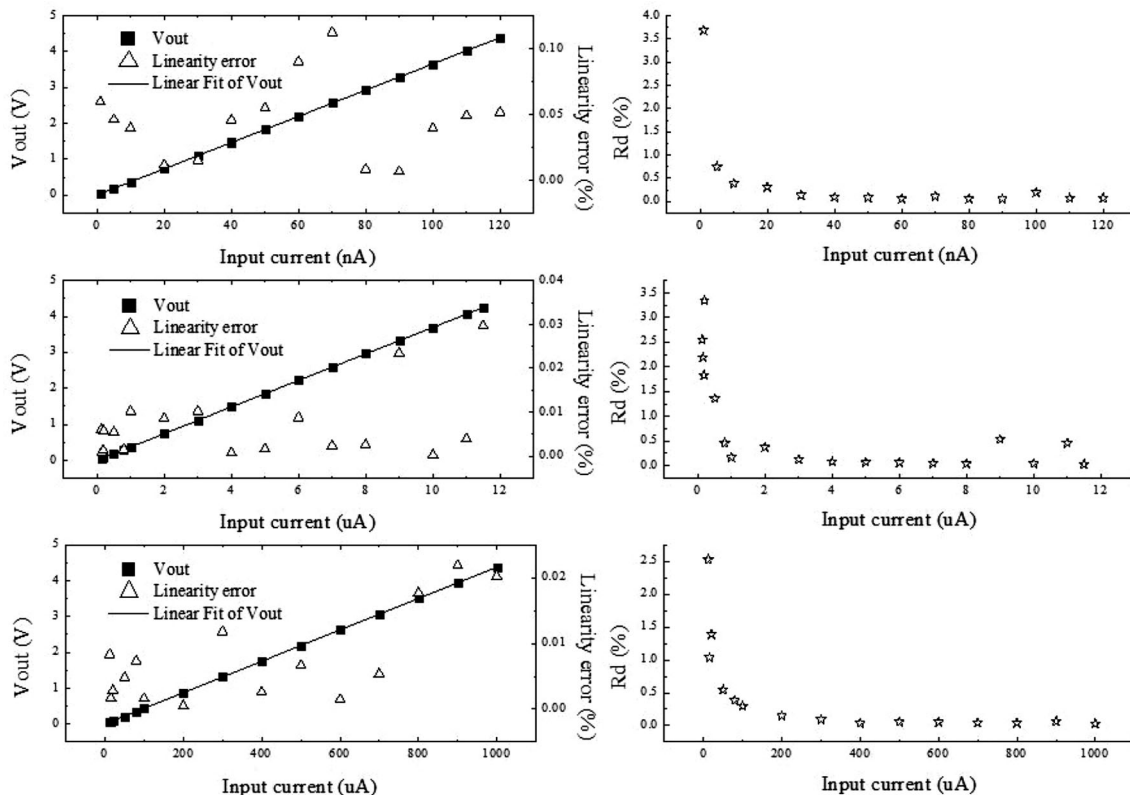
Fig. 3 Timing chart of single channel

scanner, and displays position information of the wire in real time.

4 Testing

The performance of the front-end readout electronic system was tested in a laboratory environment. The non-linearity error and resolution ($\sigma \cdot 2.36/V_{out}$) of the single channel for each measurement range are shown in Fig. 4. The nonlinearity error of the low measurement

range A (1–100 nA) was less than 0.11%, the resolution was less than 3.68%, and the absolute resolution (the difference in the fitting value and actual value) was less than 4.88 pA. The nonlinearity error of the middle measurement range B (100 nA–10 μ A) was less than 0.03%, the resolution was less than 3.34%, and the absolute resolution was less than 1.25 nA. The nonlinearity error of the high measurement range C (10 μ A–1 mA) was less than 0.02%, the resolution was less than 2.52%, and the absolute resolution was less than 0.95 nA. The test results show that the performance of the high measurement range was better

**Fig. 4** Results of nonlinearity error and resolution

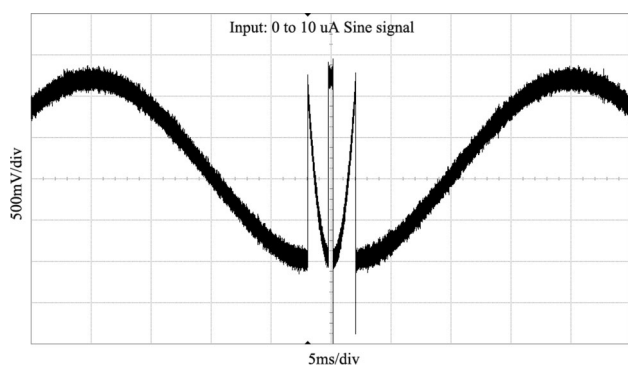


Fig. 5 Functional test results of the adaptive switch

Table 1 Parameters of the readout system

Type	Parameter value
Measurement range	1 nA to 1 mA
Full-scale differential output	10 V (± 5 V)
Event rate	1000 counts/s
Output voltage noise	< 4.6 mV (rms)
Output offset voltage	$< \pm 4.1$ mV
Nonlinearity error	$< 0.110\%$
Resolution	$< 3.68\%$
Absolute resolution	< 1.25 nA

than that of the low measurement range. The adaptive and control circuits were also tested; the magnitude of input current could be identified adaptively, and the measurement ranges of each channel could be switched correctly.

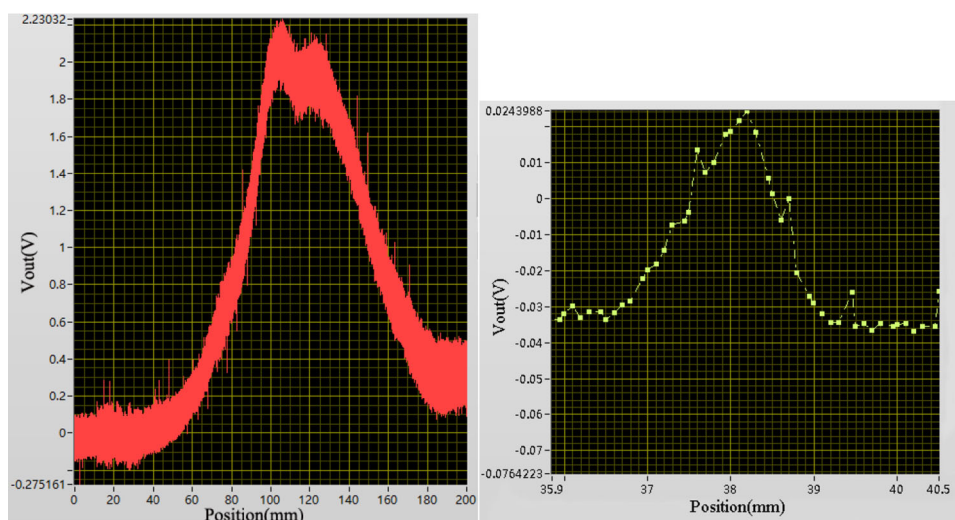
The results of the adaptive and control circuits testing are shown in Fig. 5. The horizontal axis represents time, and the vertical axis represents amplitude. The input current signal is a sine wave varying between 0 and 1 mA.

When the current was gradually reduced from 1 mA to less than $10 \mu\text{A}$, the identification and control circuit worked to switch the measurement range from the high measurement range to the middle measurement range automatically; similarly, when the current was less than 100 nA , the identification and control circuit worked to switch the measurement range from the middle range to the low range; conversely, when the current was greater than 100 nA , the identification and control circuits switched the measurement range from the low range to the middle range, and when the current was greater than $10 \mu\text{A}$, the identification and control circuits switched the measurement range from the middle range to the high range. This readout system was verified by the test results as capable of enacting the adaptive range switching function with small dead time and implementing a current measurement within a wider range.

The system was calibrated with an input current varying from 1 nA to 1 mA in the laboratory, and the performance of the system is shown in Table 1. The event rate represents the maximum frequency of the sine wave that this readout system can handle.

This system was successfully applied in the beam diagnosis of an injector II prototype for an accelerator-driven subcritical system (ADS) [15] combined with a wire scanner. The measurements of the beam profile and emittance were implemented, and the test results are shown in Fig. 6. The abscissa in this figure represents the position information, and the ordinate represents the voltage value. The first image shows the beam profile, and the second image illustrates a graph for measuring the beam emittance, for which the voltage was too small due to the placement of a slit in front of the wire scanner.

Fig. 6 (Color online) Measurement results of the beam profile and emittance



5 Conclusion

A novel fast readout system with magnitude identification and adaptive range switching was developed in this study. It is primarily used for processing signals from the wire scanner in beam diagnosis. It can be used to measure and process current signals with a Gaussian distribution and range of 1 nA–1 mA, covering six orders of magnitude, and event rates up to 1000 s^{-1} . The system can measure the beam profile and emittance and produced excellent results when applied to an injector II prototype for ADS to measure beam profile and emittance.

This proposed readout system will be instrumental in accelerator beam diagnosis systems through its ability to obtain beam quality information in real time, improvement in the accuracy of beam diagnosis, and shortening of the time required for beam tuning, which plays an important role in improving the efficiency of accelerator operation. Furthermore, the system can be widely used in nuclear physics experiments and other fields for its wide-range and weak current signal measurement [16].

Acknowledgements The authors gratefully acknowledge the staff of the Beam Feedback Department of the Institute of Modern Physics for their assistance in beam testing.

References

1. J. Sun, Y. Ruan, S. Xiao et al., Design of beam profile and halo measurement system for high-intensity RFQ accelerator. *High Power Laser Part Beams* **23**, 190–194 (2011). <https://doi.org/10.3788/hplpb20112301.0190>. (in Chinese)
2. U. Hahn, N.V. Borgen, P. Castro et al., Wire scanner system for FLASH at DESY. *Nucl. Instrum. Methods A* **592**, 189–196 (2008). <https://doi.org/10.1016/j.nima.2008.04.018>
3. A. La Rosa, M.A. Garella, F. Bourhaleb et al., A pixel ionization chamber used as beam monitor at the Institut Curie-Centre de Protontherapie de Orsay (CPO). *Nucl. Instrum. Methods A* **565**, 833–840 (2006). <https://doi.org/10.1016/j.nima.2006.06.024>
4. Y.F. Sui, L. Wang, Y. Zhao et al., BEPCII wire scanner system. *Chin. Phys. C* **34**, 1661–1664 (2010). <https://doi.org/10.1088/1674-1137/34/10/021>
5. D. Giovenale, L. Catani, L. Fröhlich, A read-out system for online monitoring of intensity and position of beam losses in electron linacs. *Nucl. Instrum. Methods A* **665**, 33–39 (2011). <https://doi.org/10.1016/j.nima.2011.11.038>
6. C.Y. Zhou, H. Su, R.S. Mao et al., An accurate low current measurement circuit for heavy iron beam current monitor. *Nucl. Instrum. Methods B* **280**, 84–87 (2012). <https://doi.org/10.1016/j.nimb.2012.01.033>
7. M. Ferrarini, V. Varoli, A. Favalli et al., A wide dynamic range BF3 neutron monitor with front-end electronics based on a logarithmic amplifier. *Nucl. Instrum. Methods A* **613**, 272–276 (2010). <https://doi.org/10.1016/j.nima.2009.11.078>
8. C.R. Rose, W. Christensen, Lisa Day et al., SNS Wire Scanner User Guide. Los Alamos National Laboratory, 11 (2002)
9. Y. Ruan, L. Han, H. Liu et al., Design and simulation of a wire scanner for the CSNS linac. *Chin. Phys. C* **34**, 1655–1660 (2010). <https://doi.org/10.1088/1674-1137/34/10/020>
10. Y. Liu, A. Aleksandrov, S. Assadi et al., Laser wire beam profile monitor in the spallation neutron source(SNS) superconducting linac. *Nucl. Instrum. Methods A* **612**, 241–253 (2010). <https://doi.org/10.1016/j.nima.2009.10.061>
11. G. Schmidt, U. Hahn, M. Meschkat et al., First results of the high resolution wire scanners for beam profile and absolute beam position measurement at the TTF. *Nucl. Instrum. Methods A* **475**, 545–548 (2001)
12. T. Yang, S. Fu, T. Xu et al., Thermal analysis for wire scanners in the CSNS Linac. *Nucl. Instrum. Methods A* **760**, 10–18 (2014). <https://doi.org/10.1016/j.nima.2014.05.061>
13. A.E. Avetisyan, S.G. Arutunian, I.E. Vasiniuk et al., Yerevan synchrotron injector electron beam transversal scan with vibrating wire scanner. *Contemp. Phys.* **46**, 247–253 (2011). <https://doi.org/10.3103/S1068337211060016>
14. Z. Xu, R. Mao, L. Duan et al., A new multi-strip ionization chamber used as online beam monitor for heavy ion therapy. *Nucl. Instrum. Methods A* **729**, 895–899 (2013). <https://doi.org/10.1016/j.nima.2013.08.069>
15. F. Yan, Z. Li, J. Tang, Preliminary physics design of China Accelerator Driven Sub-critical System main linac. *High Power Laser Part Beams* **25**, 1783–1787 (2013). <https://doi.org/10.3788/hplpb20132507.1783>
16. A. Bosco, M.T. Price, G.A. Blair et al., A two-dimensional laser-wire scanner for electron accelerators. *Nucl. Instrum. Methods A* **592**, 162–170 (2008). <https://doi.org/10.1016/j.nima.2008.04.012>